Derivation of Continuum Traffic Flow Models from Microscopic Follow-the-Leader Models.

A. Aw* A. Klar† T. Materne‡ M. Rascle§

Abstract

In this paper we establish a connection between a microscopic Follow-the-Leader model based on ordinary differential equations and a semi-discretization of a macroscopic continuum model based on a conservation law Naturally, it also turns out that the natural discretization of the conservation law in Lagrangian coordinates is equivalent to a straightforward time discretization of the microscopic model. We also show *rigorously* that, at least in the homogeneous case, the macroscopic model can be viewed as the limit of the time discretization of the microscopic model as the number of vehicles increases, with a scaling in space and time (a zoom) for which the density and the velocity remain fixed. Moreover, a numerical investigation and comparison is presented for the different models.

1 Introduction.

Microscopic modelling of vehicular traffic is usually based on so called Follow-the-Leader models, see [16, 6]. A system of ordinary differential equations is used to model the response of vehicles to their leading vehicle . These models usually consist of a system of second order ordinary differential equations. For instance (a more general nonlinearity could be considered as well) we consider

$$\begin{aligned} \dot{x}_i &= v_i, \\ \dot{v}_i &= C\frac{v_{i+1}-v_i}{(x_{i+1}-x_i)^{\gamma+1}} + A\frac{1}{T_r}\left[V(\frac{\Delta X}{x_{i+1}-x_i}) - v_i\right], \end{aligned} \tag{1}$$

where $x_i(t), v_i(t), i = 1, \ldots,$ are location and speed of the vehicles at time $t \in \mathbb{R}^+$, and ΔX is the length of a car. The basic idea is that the acceleration at time t

*Mathematiques, U Nice, France, (aaw@math.unice.fr).
†FB Mathematik, TU Darmstadt, Germany, (klar@mathematik.tu-darmstadt.de).
‡FB Mathematik, TU Darmstadt, Germany, (materne@mathematik.tu-darmstadt.de).
§Mathematiques, U Nice, France, (rascle@math.unice.fr).

depends on the relative speeds of the vehicle and its leading vehicle at time t and the distance between the vehicles. The constants $C > 0, A > 0, \gamma \geq 0$ and the relaxation time T_r are given parameters. In the *homogeneous* case $A = 0$ we recover the usual form of microscopic follow-the-leader models. For $A > 0$ a relaxation term is added, driving the velocity of the car to an equilibrium velocity V, which depends on macroscopic properties of the flow ahead of the driver. T_r is the corresponding relaxation time, different from (and typically much larger than) the reaction time of individual drivers. The constants C, γ are fitted to special situations (see [6]). A common choice is, for example, $\gamma = 0$. This case has to be treated separately from $\gamma > 0$, see below. Initial values $x_i(0) = x_i^0, v_i(0) = v_i^0$ have to be described with $v_i^0 \geq 0$ and $x_{i+1}^0 > x_i^0$. Sometimes, a time lag is included in the equations to account for the reaction times of the drivers.

Macroscopic modelling of vehicular traffic started with the work of Lighthill, Whitham and Richards[21]. They considered the continuity equation for the density ρ , closing the equation by an equilibrium assumption on the mean velocity v. The equation is

$$\partial_t \rho + \partial_x(\rho V(\rho)) \quad = \quad 0,$$

where $V = V(\rho)$ describes the dependence of the velocity with respect to the density for an *equilibrium* situation. An additional velocity equation has been introduced by Payne and Whitham in [15, 21] in analogy to fluid dynamics. Recently Daganzo [5] has pointed out some severe drawbacks of the Payne/Whitham type models in certain situations. In [2] Aw and Rascle did develop a new heuristic continuum model avoiding the above inconsistencies:

$$\begin{aligned} \partial_t \rho + \partial_x(\rho v) &= 0 \\ \partial_t(\rho v) + \partial_x(\rho v^2) - \rho^2 P'(\rho)\partial_x v &= A\,\frac{\rho}{T_r}\,[V(\rho) - v]\,, \end{aligned}$$

where $P(\rho)$ is a given function describing the anticipation of road conditions in front of the drivers, and P' denotes its derivative with respect to ρ. In [2], the authors considered the case of the homogeneous system $A = 0$, but one can also consider in particular the case $A > 0$, see [17], see also [8]. Using the new variable

$$w = v + P(\rho)$$

the model can be written in conservative form as follows :

$$\begin{aligned} \partial_t \rho + \partial_x(\rho v) &= 0 \\ \partial_t(\rho w) + \partial_x(v\rho w) &= A\,\frac{\rho}{T_r}\,[V(\rho) - v]\,. \end{aligned}$$

Initial conditions have to be prescribed : $\rho(x,0) = \rho^0(x) \geq 0$ and $v(x,0) = v^0(x) \geq 0$. We note that the coefficients in the above models can be prescribed in an a priori way or derived from microscopic considerations. See, e.g. [11] for a derivation from a kinetic traffic flow equation.

In the present paper we show how the Aw/Rascle model can be viewed as the limit of a time discretization of a microscopic Follow-the-Leader model. In particular, the macroscopic coefficient $P = P(\rho)$ is determined from the microscopic model. The paper is arranged in the following way : in Section 2 microscopic Follow-the-Leader models and the Aw/Rascle continuum model are considered in more details. In section 3 scaling limits of the microscopic equation are considered and the formal connection between microscopic and macroscopic model is established. Section 4 contains the full space-time discretization of both models and rigorous relations between the models. Section 5 considers numerically the convergence of the discretized system towards the conservation law in the limit of small time steps and large number of vehicles. We refer to [17] for a related discussion. Finally, when finishing this paper, we received from J. Greenberg - whom we thank - a very recent preprint [8], based on quite similar ideas, see Section 4.1 for some comments and a comparison of the results. We have also learnt about closely related ideas in [22]. Clearly, this kind of ideas is coming up.

2 The models.

In this section we discuss the microscopic and macroscopic models in more details.

2.1 The microscopic model.

We reconsider the microscopic equations (1) with constant $C = C_\gamma$. We introduce a new variable, the distance between say the tails of two vehicles following each other

$$l_i \;=\; x_{i+1} - x_i.$$

One obtains the system

$$\begin{aligned} \dot{x}_i &= v_i \\ \dot{v}_i &= C_\gamma \frac{(v_{i+1} - v_i)}{l_i^{\gamma+1}} + A\frac{1}{T_r}(V(\rho_i) - v_i) \end{aligned}$$

where the local "density around vehicle i" and its inverse (the local (normalized) "specific volume") are respectively defined by

$$\rho_i = \frac{\Delta X}{l_i} \text{ and } \tau_i = \frac{1}{\rho_i} = \frac{l_i}{\Delta X}$$

Remark 1
The density is often defined as the *number* of cars per unit length: here $\nu := 1/l_i$, and therefore has the dimension of the inverse of a length. With our definition, the density is already *normalized* : $\rho = \nu.\Delta X := \nu/\nu_m$, and is therefore dimensionless, so that the *maximal* density is $\rho_m = 1/\tau_m = 1$, when cars are "nose to tail". We will often write expressions like ρ/ρ_m or τ/τ_m to emphasize this normalization.

Now define the constant C_γ by

$$C_\gamma = v_{ref}(\Delta X/\ \rho_m)^\gamma = v_{ref}(\Delta X\ \tau_m)^\gamma = \ v_{ref}\Delta X^\gamma$$

where $v_{ref} > 0$ is a reference velocity, and the coefficient $(\Delta X\ \tau_m)^\gamma$ allows to recognize in (1) the derivative of function $\tilde{P}(\tau)$ defined below in (3). One obtains the microscopic model

$$\begin{aligned} \dot{x}_i &= v_i\,, \\ \dot{v}_i &= \frac{1}{\Delta X}\,(v_{i+1}-v_i)\frac{v_{ref}\tau_m^\gamma}{\tau_i^{\gamma+1}} + A\,\frac{1}{T_r}\,(V(\rho_i)-v_i)\,, \end{aligned} \tag{2}$$

where again $\tau_m = 1$ with our definition. We have

$$\dot{l}_i = v_{i+1} - v_i \ \text{ or } \ \dot{\tau}_i = \frac{1}{\Delta X}\,(v_{i+1}-v_i).$$

Using the new variable

$$w_i := \ v_i + \ \tilde{P}(\tau_i) \ \text{ with } \ \tilde{P}(\tau_i) := \begin{cases} \frac{v_{ref}}{\gamma}\ (\frac{\tau_m}{\tau_i})^\gamma & \gamma > 0 \\ -v_{ref}\ln(\frac{\tau_i}{\tau_m}) & \gamma = 0. \end{cases} \tag{3}$$

we get

$$\dot{w}_i \ = \ A\,\frac{1}{T_r}\,(V(\rho_i)-v_i)\,.$$

Altogether, one notices that equation (2) can be rewritten in the form

$$\begin{aligned} \dot{\tau}_i &= \frac{1}{\Delta X}\,(v_{i+1}-v_i) \\ \dot{w}_i &= A\,\frac{1}{T_r}\,(V(\rho_i)-v_i)\,. \end{aligned} \tag{4}$$

The initial conditions are $\tau_i(0) = \tau_i^0 > 0, v_i(0) = v_i^0 \geq 0$.

2.2 The macroscopic model.

In conservative form, the macroscopic system under consideration is given by the equations described above:

$$\begin{aligned} \partial_t\rho + \partial_x\rho v &= 0, \\ \partial_t\rho w + \partial_x v\rho w &= A\,\frac{\rho}{T_r}\ [V(\rho)-v] \end{aligned} \tag{5}$$

where ρ is again defined as the (normalized) density, i.e. the (local) dimensionless fraction of space occupied by the cars, and v denotes the macroscopic velocity of the

cars. Moreover, $A = 0$ in the case of the homogeneous model and A is a positive constant, say $A = 1$ for the relaxed model, and

$$w = v + P(\rho). \tag{6}$$

The hyperbolic part of the above system writes :

$$\begin{aligned} \partial_t \rho + \partial_x(\rho v) &= 0 \\ \partial_t(\rho w) + \partial_x(v\rho w) &= 0. \end{aligned} \tag{7}$$

In the following, we consider a special class of functions $P(\rho) := \tilde{P}(1/\rho)$, where $\tilde{P}$ is defined in (3). In other words, for $\rho > 0$,

$$P(\rho) = \begin{cases} \frac{v_{ref}}{\gamma}\left(\frac{\rho}{\rho_m}\right)^\gamma, & \gamma > 0, \\ v_{ref} \ln\left(\frac{\rho}{\rho_m}\right), & \gamma = 0, \end{cases} \tag{8}$$

where, as in the previous Subsection, $\rho_m = 1$ and v_{ref} is a given reference velocity. The function P is not a pressure. In fact, it is homogeneous to a velocity, [11], [17]. In the context of gas dynamics - completely irrelevant here, see [5], [2]- this pseudo-pressure P would be homogeneous to the enthalpy, so that the exponent γ here plays the role of the usual $(\gamma - 1)$. In particular, the case $\gamma = 0$ here would correspond to the isothermal case, with the same mathematical advantages and difficulties : e.g. one of the Riemann invariants is unbounded near regions of local vacuum, see further. To obtain a well defined problem for the case with relaxation : $A > 0$, we choose the function $V = V(\rho), \rho > 0$, such that

$$-P'(\rho) \leq V'(\rho) \leq 0 \tag{9}$$

is fulfilled for all $\rho > 0$. This is the so-called *subcharacteristic condition*, see e.g. [21], [3], [7]. A typical choice would be $V(\rho) = -c\,(P(\rho) - P(\rho_m))$, $0 \leq c \leq 1$, and a description of the equilibrium curve $v = V(\rho)$ in the (w, v) plane is shown in Figure 1, (left), for the case $\gamma > 0$, and in Figure 2,(left) for $\gamma = 0$. Of particular interest is the *characteristic* case , where the equality holds in one of the above inequalities. More precisely, if $\gamma > 0$, we assume that

$$V'(\rho) = -P'(\rho) \text{ (resp. } 0) \text{ for } \rho \leq \rho_* (\text{ resp. } \rho_* \leq \rho \leq \rho_m), \tag{10}$$

where ρ_* is some positive intermediate value between $\rho = 0$ and the maximal value ρ_m of ρ. The equilibrium curve is shown in Figure 1, (right), see [17].

In contrast, if $\gamma = 0$, then in the characteristic case we will assume that

$$\begin{aligned} V(\rho) = v_m \text{ (resp. } -P(\rho) \text{) (resp. } 0 \text{)} \\ \text{for } 0 \leq \rho \leq \rho_* \text{ (resp. } \rho_* \leq \rho \leq \rho_{**} \text{) (resp. } \rho_{**} \leq \rho \leq \rho_m \text{),} \end{aligned} \tag{11}$$

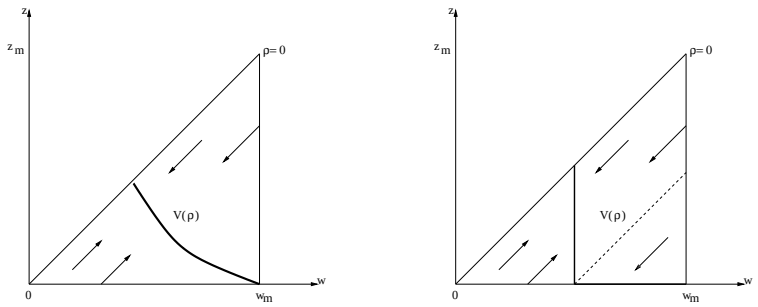

Figure 1: Invariant region R and equilibrium curve $v = V(\rho)$ for $\gamma > 0$, in the $(w, z) = (w, v)$ plane, in the subcharacteristic case (left), and in the characteristic case (right). In the first case, the convexity of the equilibrium curve could be arbitrary.

where ρ_* and ρ_{**} are two positive intermediate densities, see Figure 2 (right). In this case $\gamma = 0$, Figures 3 show examples of the *same* equilibrium curve and associated bounded region (in the $(\rho,\ \rho\, v)$ plane), which are *invariant* for the *full* system (5), in the *subcharacteristic* case Figure 3, (left), and in the *characteristic* case Figure 3, (right).

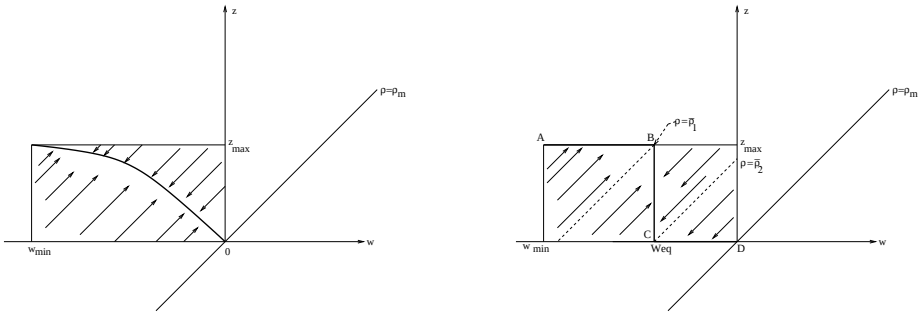

Figure 2: Invariant region R and equilibrium curve $v = V(\rho)$ for $\gamma = 0$, in the (w, v) plane, in the subcharacteristic case (left), and in the characteristic case (right).

Moreover, let $\tau := \rho^{-1}$ be the specific volume, and define the associated functions

$$\tilde{P}(\tau) = P(\frac{1}{\tau})\ ,\ \tilde{V}(\tau) = V(\frac{1}{\tau})\ ,\ w = v\ +\ \tilde{P}(\tau). \tag{12}$$

We note that

$$\tilde{P}'(\tau) = -\frac{v_{ref}\tau_m^{\gamma}}{\tau^{\gamma+1}}, \gamma \geq 0$$

where $\tilde{P}'$ denotes the derivative of $\tilde{P}$ with respect to τ and, as in Remark 1, $\tau_m := \rho_m^{-1} = 1$. For $\rho > 0$ we have $\tilde{P}' < 0$ and $\tilde{P}'' > 0$. For $\rho > 0$, using the specific volume

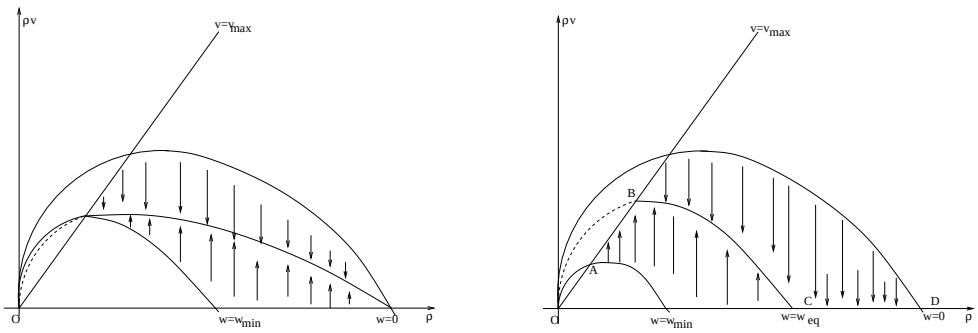

Figure 3: Invariant region R and equilibrium curve $v = V(\rho)$ for $\gamma = 0$, in the $(\rho,\ \rho\ v)$ plane, in the subcharacteristic case (left), and in the characteristic case (right).

τ, we now transform (5) : we change the Eulerian coordinates (x,t) into Lagrangian "mass" coordinates (X,T), see [4], with

$$\partial_x X = \rho,\ \partial_t X = -\rho v,\ T = t$$

or

$$\partial_X x = \rho^{-1} = \tau,\ \partial_X t = 0,\ \partial_T x = v,\ \partial_T t = 1.$$

Thus, $X = \int^x \rho(y,t)dy$ is not a mass. In fact, it describes the total space occupied by cars up to point x. We obtain

$$\begin{aligned} \partial_T \tau - \partial_X v &= 0\ , \\ \partial_T w &= A\,\frac{1}{T_r}\,[V(\rho) - v]\ . \end{aligned} \tag{13}$$

Since $w = v + \tilde{P}(\tau)$, this is a hyperbolic system to the unknown functions w and τ, with relaxation term if $A > 0$. We add initial conditions $\tau^0(x) > 0$ and $v^0(x) \geq 0$. We note that, as in the case of gas dynamics, [20], even for *weak* (L^∞) solutions, this new system is equivalent to (5). This equivalence holds *even* in the vacuum case, where the map $x \to X$ is not invertible, so that $\partial_X x = \tau$ contains a delta-function. However, in this case one must admit for (13) a larger class of test-functions, which is an additional difficulty. In the numerical schemes described below, each cell moves between two trajectories, so that the total mass inside this cell remains constant. Therefore in each nonvoid cell, the (usual) weak solutions to (5) and (13) are the same.

3 Scaling and formal macroscopic limit of the microscopic equations.

According to (4) the microscopic system can be written as

$$\begin{aligned} \dot{\tau}_i &= \frac{1}{\Delta X}(v_{i+1} - v_i), \\ \dot{w}_i &= A\,\frac{1}{T_r}\left(V(\rho_i) - v_i\right), \end{aligned}$$

where $w_i = v_i + \tilde{P}(\tau_i)$ is defined in (3). On the other hand, denoting time by t as in Eulerian coordinates, the Lagrangian macroscopic system (13) rewrites

$$\begin{aligned} \partial_t \tau &= \partial_X v, \\ \partial_t w &= A\,\frac{1}{T_r}\left[V(\rho) - v\right], \end{aligned}$$

with again $w = v + \tilde{P}(\tau)$. Clearly, (4) is at least a rough *semi*-discretization of (13). Let us now introduce the scaling. Obviously a macroscopic description for traffic flow is only valid if we consider a large number of vehicles on a long stretch of the highway. Therefore we introduce a scaling such that the size of the domain under consideration is going to infinity, as well as the number of vehicles, whereas the length of cars is shrinking to 0.
In other words, we "make a zoom", i.e. we introduce a small parameter ε, and we multiply the space and time units by $1/\varepsilon$, i.e. we shrink space and time coordinates x and t to

$$x' := \varepsilon\, x \text{ and } t' := \varepsilon\, t.$$

In particular the length of a car is now $\Delta X' := \varepsilon.\Delta X$.
Practically, the parameter ε is proportional to the inverse of the maximal possible number of cars per (new) unit length. The space and time derivatives are muliplied by ε. Similarly, since X is the primitive of ρ in x, it is replaced by $X' := \varepsilon\ X$, and therefore the derivatives in X are also multiplied by ε. On the other hand, the normalized density and specific volume are unchanged, as well as the velocity and the other Riemann Invariant $w = v + \tilde{P}(\tau)$:

$$\rho' = \rho\ ,\ \tau' = \tau\ ,\ v' = v\ ,\ w' = w.$$

Dropping the primed notation for these unchanged dependent variables, system (13) becomes :

$$\begin{aligned} \frac{\partial \tau}{\partial t'} &= \frac{\partial v}{\partial X'}\,, \\ \frac{\partial w}{\partial t'} &= A\,\frac{1}{\varepsilon\, T_r}\left[V(\rho) - v\right]. \end{aligned} \tag{14}$$

Now let us look at the microscopic system, with the same scaling. The only additional modification is : $l_i' = \varepsilon\, l_i$, and the relation $\tau_i = l_i/\Delta X$ is preserved with the primed variables. Dropping again the primes for the unchanged dependent variables, system (4) becomes

$$\begin{aligned} \frac{d\tau_i}{dt'} &= \frac{1}{\Delta X'}(v_{i+1} - v_i) \\ \frac{dw_i}{dt'} &= \frac{A}{\varepsilon\, T_r}\ (V(\rho_i) - v_i)\,. \end{aligned} \tag{15}$$

Now let us discuss the consequences of the above scaling on the *equations.* There are two cases.

A. The homogeneous case $A = 0$. In this case, not suprisingly, the hyperbolic system and the microscopic system remain unchanged with this self-similar scaling. The only (important !) difference is that in the new coordinates, the mesh size (see the next Section) : $\Delta X' = \varepsilon \Delta X$ tends to 0 when the zoom parameter ε tends to 0.
Therefore, at least *formally,* the microscopic system "converges" to the macroscopic one when ε tends to 0. More precisely, in this homogeneous case $A = 0$, (15) can be viewed as the natural semi-discretization of (14), see Section 4, finer and finer when ε tends to 0. Obviously, the scaling changes the *initial data*, see Remark 3 below.

B. The relaxed case $A > 0$. Then there are two possibilities :
(i) First, assume that the positive constant A in front of the relaxation time depends nicely on some macroscopic scale, and in fact is proportional to ε.
In other words, let us assume that the relaxation time is comparable in size to the number of cars per (rescaled) unit length. We note that for numerical purpose, we do not really need to let ε tend to 0, but we only need to consider a "small" ε, so that the semi-discretization (15) is "fine enough", see Remark 2 below. In this case, the conclusion is the same as in the homogeneous case: the macroscopic system is at least the *formal* limit of the microscopic one.
(ii) On the contrary, assume that this constant A is unchanged in the scaling, then we formally end up with a scalar Lighthill-Whitham-Richards type equation, but then the limit we are considering is the limit $(\Delta X', \Delta t') = (\Delta X, \Delta t)\ \varepsilon \to\ (0, 0)$, with ΔX and Δt constant.

Remark 2
The size of the physical quantities allows for various possibilities to scale nicely the equations, with relatively small (but *finite*) values of ε, possibly with *different* scaling constants in x and t. For instance, assume that the "old" units are meter and second. Then, choose as "new" units (or reference length and time) 1500 m (or a mile) and 1 minute, with $\Delta X = 5$ m. Then rescale as follows :

$$x' = \frac{x}{1500}\ ,\ t' = \frac{t}{60}.$$

On the other hand, a typical velocity is 90 km/h, i.e. 25 m/s, or 1500 m per mn, i.e. 1 in the new units, which is perfect. Moreover, in these new units, the length of a car is $\Delta X' = 5/1500 = 1/300$, whereas a good time step in the time discretization, of the same order as the reaction time of the drivers, would be $\Delta t = 1/5$ second $= 1/300$ of the new time unit. Thus, in such a system of units, a typical (maximal ?) velocity is of order 1, as well as the maximal (normalized) density, whereas typical space and time steps are of the order of $1/300$ of the corresponding unit, subject of course to the CFL condition, see the next Section. On the other hand, the relaxation time is typically found to be around 30 seconds, i.e. 0.5 in the new units, see for example [12]. In such a scaling, the rescaled relaxation time , i.e. $\frac{A}{\varepsilon T}$ would still remain *finite*, and therefore we would still be far away from the zero-relaxation limit, i.e. from the Lighthill-Whitham-Richards model.

Remark 3
So far, we have not discussed the problem of the *initial data.* Let us restrict ourselves to the *homogeneous* case $A = 0$, say in Lagrangian coordinates (the discussion would be the same in Eulerian coordinates). In this case, as we said, the scaling preserves the system (13) (with $A = 0$), which we rewrite in the general form

$$\frac{\partial U}{\partial t'} + \frac{\partial F(U)}{\partial X'} = 0, \tag{16}$$

with $U := U^\varepsilon := (\tau^\varepsilon,\ w^\varepsilon)$. However, this scaling modifies the initial data, where there are obviously (at least) two scales : the microscopic one, i.e. the length of a car (a few meters), and the macroscopic one (say one kilometer). Therefore, it is natural to extend the microscopic initial data defined in Section 2.1, and to assume for instance that in rescaled Lagrangian coordinates the initial data write :

$$U_0^\varepsilon(X') = \sum_j \overline{U_j^0}\chi_j(X'), \tag{17}$$

where the characteristic function χ_j satisfies : $\chi_j(X') = 1$ iff $X' \in I_j := (X'_{j-1/2},\ X'_{j+1/2})$, with $X'_l := l\Delta X'$, and $\overline{U_j^0}$ is the average value of a "macroscopic" function U_0 over the same interval.

When $\varepsilon \to 0$, the initial data (17) provide initial numerical data to approximate the solution of the initial value problem (16), (18), with

$$U(X', 0) = U_0(X'). \tag{18}$$

4 Rigorous relations between the microscopic and macroscopic equations.

4.1 The discretized models.

In this section we will show that a standard explicit Euler discretization of the microscopic model is equivalent to the classical Godunov scheme applied to the macroscopic model. Moreover, this discretization is investigated in more detail.

The discretized microscopic model.

We first introduce an explicit Euler time discretization of the *new* microscopic model, (15) using the *rescaled* time step $\Delta t'$. With the above scaling we note that the *new* Δt and ΔX tend to zero when ε tends to 0, with a *fixed* ratio $\lambda := \Delta t/\Delta X$. Neglecting the primed notation, i.e.writing Δt and ΔX instead of $\Delta t'$ and $\Delta X'$, we obtain :

$$\tau_i^{n+1} = \tau_i^n + \frac{\Delta t}{\Delta X}(v_{i+1}^n - v_i^n), \tag{19}$$

with

$$v_i^{n+1} = w_i^{n+1} - \tilde{P}(\tau_i^{n+1}),$$

and if $A > 0$ the relaxation is approximated by

$$w_i^{n+1} = w_i^n e^{\frac{-A\,\Delta t}{\varepsilon T_r}} + (\tilde{V}(\tau_i^{n+1}) + \tilde{P}(\tau_i^{n+1}))(1 - e^{\frac{-A\,\Delta t}{\varepsilon T}}), \tag{20}$$

with $\rho_i^n = 1/\tau_i^n$. Of course, formula (20) contains the homogeneous case : if $A = 0$, then

$$w_i^{n+1} = w_i^n. \tag{21}$$

On the other hand, if $A > 0$ the relaxation term is correctly treated for ε small, i.e. for small relaxation times, where the equations are becoming stiff. Now let us discretize the macroscopic model.

The discretized macroscopic model.

As above, we consider the macroscopic model (14) in rescaled variables x', t', with corresponding steps $\Delta t'$, $\Delta X'$, and we drop again the primed notations. Then (14)

is discretized using a splitting scheme which treats separately the convection and the relaxation terms. Consider

$$\begin{aligned} \partial_t \tau - \partial_X v &= 0 \\ \partial_t w = 0\,, \quad &\text{if } A = 0, \end{aligned} \tag{22}$$

and

$$\partial_t w = \frac{A}{\varepsilon T}\left[V(\rho) - v\right]\,, \quad \text{if } A \neq 0. \tag{23}$$

The most natural discretization to treat the convection part is the Godunov scheme. The relaxation part is treated by the same time discretization as for the microscopic model. Before writing Godunov's method for the hyperbolic equation, we need a brief description of the solution to the Riemann Problem:
We consider the system (22), or the equivalent system (7) in Eulerian coordinates. We recall that $w = v + \tilde{P}(\tau)$. First, the eigenvalues of the system (22) are $\lambda_1 = \tilde{P}'(\tau) < 0$ and $\lambda_2 = 0$. The Riemann invariants are w and $z := v$. They satisfy for smooth solutions

$$\partial_t v + \lambda_1 \partial_x v = 0\,; \partial_t w + \lambda_2 \partial_x w = 0.$$

Now, since $\tilde{P}''(\tau) > 0$, it turns out that the first eigenvalue λ_1 is genuinely nonlinear (GNL), i.e. $\forall (w,v), \partial\lambda_1/\partial v \neq 0$. On the contrary, $\partial\lambda_2/\partial w \equiv 0$, i.e. $\lambda_2 = 0$ is linearly degenerate (LD), as for the original system (7) in Eulerian coordinates.
Now let us denote the left and right Riemann data by (w_L, v_L) and (w_R, v_R) respectively. Since the first characteristic speed is genuinely nonlinear, a state (w,v) can be connected on its left (in the (X,T) plane) to (w_L, v_L), either by a backward 1-shock if $v < v_L$, which corresponds to *braking*, or by a backward 1-rarefaction (acceleration) wave if $v > v_L$.
Moreover, see [2], these equivalent systems (7) and (22) are sometimes called *Temple* systems, [19], see also [10] : their shock curves and rarefaction curves coincide. Therefore, *even in the case of a shock*, we have $w = w_L$.
On the other hand, (w,v) can be connected on its right to (w_R, v_R) by a stationary 2-contact discontinuity $v = v_L$. Hence, two states (w_L, v_L) and (w_R, v_R) can be connected through a constant intermediate state (w_0, v_0), which is connected to (w_L, v_L) by a 1-shock (braking) if $v_R < v_L$, or on the contrary by a (continuous) 1-rarefaction wave (acceleration) if $v_R > v_L$ and to (w_R, v_R) by a 2-contact discontinuity. Moreover, w, v are monotone functions of X/t for all values of this variable, whereas τ is only monotone inside *each* elementary wave. In general, $(w_0, v_0) := (w_L, v_R)$, so that we can easily solve graphically the Riemann Problem in the coordinates of Figure 1 or 2.

Proposition 1
We consider here the system (22), or the equivalent system (7) in Eulerian coordinates, with the above data (w_L, v_L) and (w_R, v_R). Then

(i) No local extremum of w or v is created for $t > 0$. Therefore the *total variation* in space of *each* Riemann Invariant is *nonincreasing* in time. More precisely,

$$|f_+ - f_0| + |f_0 - f_-| = |f_+ - f_-| \ , \ f := w \text{ or } v.$$

(ii) In the case $\gamma > 0$, the density is nonnegative if and only if $w - v = P(\rho) \geq 0$. Consequently, the intermediate state is at *vacuum* if the cars in front are "too fast" with respect to the following cars, namely if

$$v_R > w_L = v_L + \tilde{P}(\tau_L).$$

In this case, $\rho = 1/\tau = 0$, v and w are not physically defined, but if we insist and *mathematically* define for instance $v_0 = w_0 = w_L$, then statement (i) remains true.
(iii) In the same case $\gamma > 0$, any region defined by the Riemann invariants :

$$\mathcal{T} := \{0 \leq v \leq w \leq w_m = P(\rho_m)\},$$

is *bounded* and *invariant* for the Riemann Problem, and corresponds to bounded nonnegative densities and velocities. An example of such a region is the triangle represented in Figure 1. Moreover, any rectangle

$$\mathcal{R} := \{(w, v); 0 \leq w_{min} \leq w \leq w_m = P(\rho_m) \ , \ 0 \leq v_{min} \leq v \leq v_{max}\} \tag{24}$$

inside $\mathcal{T}$ is also *invariant* for the Riemann Problem, away from vacuum if $w_{min} - v_{max} > 0$.
(iv) In the case $\gamma = 0$, vacuum corresponds to $w = -\infty$. Therefore, *any* rectangle

$$\mathcal{R} := \{-\infty < w_m \leq w \leq 0 \leq v \leq v_m\}, \tag{25}$$

is *invariant* for the Riemann Problem, corresponds to bounded nonnegative velocities and densities bounded from below by *positive* quantities.

Proof :
Statements (ii) and (iii) are related to the case $\gamma > 0$, which has been studied in detail in [2]. Statement (i) is then obvious, including if vacuum appears.
Now, let us consider the case $\gamma = 0$, which is often considered in the literature on microscopic models, see e.g. [16], [6]. In this case, it is also easy to check statement (iv), using again the relations $w_0 = w_- \ , \ v_0 = v_+$. So the proof is complete. □

Remark 4
In the case $\gamma = 0$, when solving the Riemann Problem, it i easy to check that the maximal possible speed that cars can reach in an acceleration wave emanating from (w_L, v_L) is infinite. Therefore, the cars behind can always catch up with the cars in front of them, without having to reach the vacuum, compare the numerical results in Figures 5 and 6 in Section 5 below. □

Now (22) is discretized using the Godunov method for the hyperbolic problem: We introduce grids in time and mass coordinate with (rescaled) stepsize Δt and ΔX and grid points t_n and $X_{i+1/2}$. Let f_i^n denote the approximation of the function $f(t,X)$ for $X \in [X_{i-1/2}, X_{i+1/2}), t \in [t_n, t_{n+1})$. Let $\lambda = \frac{\Delta t}{\Delta X}$ be the grid ratio.
In view of the above discussion the Godunov method for system (22) is given by

$$\begin{aligned} w_i^{n+1} &= w_i^n \\ \tau_i^{n+1} &= \tau_i^n + \lambda(v_{i+1/2}^n - v_{i-1/2}^n) \\ &= \tau_i^n + \lambda(v_{i+1}^n - v_i^n). \end{aligned} \tag{26}$$

And if $A \neq 0$ the full discretization is then

$$\begin{aligned} \tau_i^{n+1} &= \tau_i^n + \lambda(v_{i+1}^n - v_i^n), \\ w_i^{n+1} &= w_i^n e^{\frac{-A\ \Delta t}{\varepsilon T_r}} + (V(\rho_i^{n+1}) + P(\rho_i^{n+1}))(1 - e^{\frac{-A\ \Delta t}{\varepsilon T_r}}), \end{aligned} \tag{27}$$

so that we recover exactly the above system (20)(or (19) when $A = 0$). We have therefore shown the equivalence between the discretisations of the microscopic and the macroscopic system.
By the way, in the macroscopic view of this scheme it will be clear in Theorem 1 below that the (sub)characteristic condition is necessary for the stability. This is far from being obvious in the microscopic interpretation.
Classically, the above numerical scheme consists of three successive steps, described here in Lagrangian coordinates for nonvoid cells:
1. Starting from piecewise constant data $U_i^n := (\tau_i^n, w_i^n)$ in each cell, solve the Riemann Problem, for $t_n < t < t_{n+1}$ assuming that the CFL condition is satisfied. Let $U_h(X,t) := (\tau_h, w_h)(X,t)$ denote the corresponding solution. In fact the index h stands for the couple $(\Delta X, \Delta t)$, and plays the role of the scaling parameter ε in Section 3. We note that the intermediate state $U_{i+1/2}^n$ in the Riemann Problem satisfies

$$w_{i+1/2}^n = w_{i+1/2}^n\ ,\ v_{i+1/2}^n = v_{i+1}^n. \tag{28}$$

2. At time t_{n+1}, average this solution on each cell, i.e. solve (19). If $A \neq 0$ let us denote the average values of conservative variables by $(\tau_i^{n+1/2}, w_i^{n+1/2})$.
3. If $A \neq 0$, approximate the ordinary differential equation as above, to obtain $(\tau_i^{n+1}, w_i^{n+1})$ from (27).

Again, the formulas would be the same in Eulerian coordinates, except that now the cells $x_{i-1/2}, x_{i+1/2}$ would be moving with time. Since $v_{i+1/2}^n = v_{i+1}^n$ we refresh the position by :

$$x_{i+1/2}^{n+1} = x_{i+1/2}^n + \Delta t v_{i+1}^n.$$

Now let $I(a,b) := [\min(a,b), \max(a,b))$. Using Proposition 1 and standard ideas, we obtain the first important result :

Theorem 1
We consider the above algorithm, under the CFL condition, assuming if $A \neq 0$ that the (sub)characteristic condition is satisfied, and that the initial data lie in an invariant rectangle $\mathcal{R}$, away from vacuum. Then
(i) We first assume that $A = 0$. Then, as in Proposition 1, in each Riemann Problem the total variation of w_h is nonincreasing in time. Moreover, in each cell, w_h remains constant : $w_h(x,t) \equiv w_i^n$. Consequently v_h and also τ_h are monotone in each cell. Moreover, $(w_h(X,t), v_h(X,t))$ remains in the invariant region $\mathcal{R}$ for $t_n \leq t \leq t_{n+1}$.
(ii) In step 2, $w_i^{n+1/2} = w_i^n$. On the other hand, since in each cell w_h is constant and τ_h monotone, the average $\tau_i^{n+1/2}$ is in $I(\tau_i^n, \tau_{i+1/2}^n)$. By monotonicity the same result is true for the velocity. In fact,

$$v_i^{n+1/2} \in I(v_i^n, v_{i+1/2}^n) = I(v_i^n, v_{i+1}^n).$$

(iii) Finally, the invariant rectangle $\mathcal{R}$ is also invariant for the Godunov scheme. Moreover the total variation in space of the Riemann Invariants : $\sum_j |f_{i+1}^n - f_i^n|$, $f = w$ or v is still decreasing with respect to n. Since w_h is constant and v_h monotone in each cell, the total variation in *time* of w_h and of $\tilde{v}_h : (x,t) \to v_i^n + \Delta t(v_i^{n+1} - v_i^n)$ is also controlled from above.
(iv) On any time interval (t_n, t_{n+1}) the solution U_h, satisfies the (discrete) *entropy inequality* in the sense of Lax : for any convex entropy $\eta(U) = \eta(\tau, w)$ associated to the entropy flux $q(U)$, and for any n and j,

$$\eta(U_j^{n+1}) \leq \eta(U_j^n) - (\Delta t/\Delta X)(q(U_{j+1/2}^n) - q(U_{j-1/2}^n)). \tag{29}$$

v) Now we consider the full problem, and we assume that the invariant rectangle $\mathcal{R}$ is constructed as in Figure 1 or 2 : e.g. in the subcharacteristic case its upper left and lower right corner are at equilibrium. Then the region $\mathcal{R}$ is also invariant by (13, ii) and by step 3, i.e. by (20). Moreover, under the (sub)characteristic assumption, the *sum* of the total variations in space of the Riemann Invariants : $\sum_j (|w_{j+1}^n - w_j^n| + |v_{j+1}^n - v_j^n|)$ is still nonincreasing in time, and the other conclusions of (iii) remain valid for (20). Consequently, since the inverse function $\tilde{P}^{-1}$ is Lipschitz (away from vacuum), the total variation of τ_h also remains uniformly bounded in time.

Sketch of Proof.
Statements (i) to (iii) exploit in particular the monotonicity of v between v_j^n and v_{j+1}^n, which is obvious since w_h is constant in each cell, so that there is only one simple wave per cell. Note that v is not a conserved variable, so that an *Eulerian* classical Godunov scheme the averaging step would *not* preserve the total variation and the invariant regions.
Statement (iv) is classical : on any time interval (t_n, t_{n+1}) the solution U_h is constructed by the Riemann Problem and thus satisfies the *entropy inequality* in the sense of Lax, [13]. Therefore, by Jensen inequality, the new average values U_j^{n+1}

satisfy (29).
Finally, besides the above-mentioned references, it is an exercise to show (v) : indeed, in (27), compute the differences $(w_{i+1}^{n+1} - w_i^{n+1})$ and $(v_{i+1}^{n+1} - v_i^{n+1})$ in terms of the previous values $f_j^{n+1/2}$, $f = w$ or v, multiply each difference by its sign and add them. Then use the (sub)characteristic assumption to show the result. In the *characteristic* case, see [8], we note that the evolution of w in each cell does *not* depend on the other cells, so that the total variation of each Riemann invariant w and v is nonincreasing in time, whereas in the subcharacteristic case, see [1],[14], we can only control the *sum* of these total variations. □

4.2 Convergence results and hydrodynamic limit.

There are three levels of description : the fully discrete system (27), or (19), (21), the Follow-the-Leader model (1), and the continuous system (22). In this section we discuss first the limit from the fully discrete level (26) to the continuous macroscopic model. Moreover, passing from the fully discrete level (26) to the semi- discrete one (1), and passing from the latter to the continuous level (22) is considered.
With the above scaling, we *state* a first *rigorous* result of convergence of the Godunov scheme when $\varepsilon \to 0$. I.e. we state a result dealing with the limit of (26) to (22) when the rescaled Δt and ΔX tend to 0 with a fixed ratio λ fixed, fulfilling the CFL condition.
For simplicity, we consider the *homogeneous* case $A = 0$, away from vacuum, and we state the result in *rescaled* Lagrangian coordinates, dropping again the primed notations. However, our result is also valid for system (14), in rescaled variables, in the (less realistic) case where A is proportional to ε, i.e. $A_0\ \varepsilon$ instead of A. Similarly, the result is also the same for the two corresponding systems in *Eulerian* coordinates. Using the above and standard compactness results, as well as standard results to control the error in the projection steps, we obtain :

Theorem 2
Let us consider the rescaled initial data (18), and assume that the associated Riemann invariants w_0 and v_0 are bounded, have a bounded total variation, and lie in an invariant rectangle $\mathcal{R}$, away from vacuum.
Then, using the piecewise-constant initial data (17) as initial data for this scheme, at least a subsequence $U_h := (w_h, \tau_h)$ produced by the numerical scheme (19) converges to a weak entropy solution to the initial value problem (16), (18) as the rescaled Δt and ΔX tend to 0 with a fixed ratio λ, fulfilling the CFL condition, as the zoom parameter $\varepsilon \to 0$.

The above result deals with passing directly from (26) to (22).
It strongly suggests studying the two other natural limits : passing from the fully

discrete level (26) to the semi- discrete one (1), and passing from the latter to the continuous level (22).
Again we restrict ourselves to the case $A = 0$, away from vacuum.

Theorem 3
Under the above assumptions, i.e. $A = 0$, and the initial data lie in an invariant rectangle $\mathcal{R}$, away from vacuum, we consider in Lagrangian coordinates the values $U_i^n := (\tau_i^n, w_i^n)$ constructed by (26) or (19), (21), but now we only rescale the time step. Therefore the rescaled time step Δt vanishes, with a *fixed* space mesh size ΔX. Moreover, we assume that the initial data are constant for X large enough, so that there is a "first" car. Then
(i) The Initial Value Problem (IVP) for the (infinite) Follow-the-Leader system (1) (with $A = 0$), has a unique solution $U(t)$, defined at least locally in time. Its natural first order approximation (19), (21) is stable and consistant, and therefore the whole sequence is convergent, for any *fixed* ΔX.
(ii) The values U_i^n stay in the invariant bounded region $\mathcal{R}$, and satisfy the uniform BV estimates as in Theorem 1. Consequently, the solution U of (1) is globally defined and satisfies the same uniform estimates.
(iii) Moreover, set $U_i := (\tau_i, w_i)$ and let
$F_{i+1/2} := G(U_i, U_{i+1}) := F(U_{i+1/2}) = F(U_{i+1}) := (v_{i+1},\ 0) = (w_{i+1} - \tilde{P}(\tau_{i+1}),\ 0)$
denote the (well defined) Godunov flux at the interface $X = X_{i+1/2}$. This nonlinear relation is preserved in the limit $\Delta t \to 0$: for all $t \geq 0$, $F_{i+1/2}(t) := G(U_i(t), U_{i+1}(t)) = (v_{i+1},\ 0) = F(U_{i+1}(t))$. Finally (1) is the semi-discretisation of (22): for any $t \geq 0$,

$$\frac{dU_i}{dt}(t) = -(\Delta X)^{-1}\ (F_{i+1/2}(t) - \ F_{i-1/2}(t)). \tag{30}$$

Sketch of Proof. The first part of this result can be adapted from standard textbooks (see e.g. [18]) to the case of infinite- dimensional systems of Ordinary Differential Equations, here with the l^∞ norm. The other results use the discrete BV estimates (in space and in time) inherited from the Godunov scheme. □

Now, define $\mathcal{U}_h(X, t) := \sum_j (\tau_i(t), w_i(t))\ \chi_i(X)$, where χ is defined as in (17).

Theorem 4
Under the same assumptions as in Theorem 3, consider the IVP for the Follow-the-Leader system (1) (with $A = 0$), and let ΔX tend to 0.
Then at least a subsequence of the sequence $\mathcal{U}_h$ converges boundedly almost everywhere to an entropy weak solution $U := (\tau, w)$ to the macroscopic system : (22) for

any smooth $\phi(X,t)$ with compact support,

$$\int_0^{+\infty} \sum_i \int_{I_i} [\, U(X,t)\ \partial_t \phi(X,t) \ +\ F(U(X,t))\ \partial_X \phi(X,t)]\ dX\ dt$$
$$+ \sum_i \int_{I_i} U_0(X)\ \phi(X,0) dX := A + B + D \ =\ 0, \tag{31}$$

and similarly the entropy inequality in the sense of Lax holds for any convex entropy.

Sketch of Proof. Multiply (30) by an arbitrary test-function $\phi(X,t)$, make a (discrete) integration by parts in X and t, and let ΔX tend to 0. We obtain, for any smooth function $\phi(X,t)$ with compact support contained in $[-L,L]x[0,T]$:

$$\int_0^{+\infty} \sum_i \int_{I_i} [\, U_i(t) \partial_t \phi(X,t) \ + (\Delta X^{-1}) F_{i+1/2}(t))(\phi(X+\Delta X,t) - \phi(X,t))] dX dt$$
$$+ \sum_i \int_{I_j} U_i(0) \phi(X,0) dX \ := A_h + B_h + D_h = 0. \tag{32}$$

By compactness, A_h and D_h respectively tend to A and D when $h \to 0$. As to B_h, with an obvious first order Taylor expansion, we see that for any ϕ, $|B_h - E_h| \leq C\ \Delta X$, where

$$E_h := \int_0^{+\infty} \sum_i \int_{I_i} F_{i+1/2}(t) \partial_X \phi(X,t) dX dt,$$

and C depends on the L^∞ norm of $F(U)$ and on $L\ T ||\partial_X^2 \phi||_\infty$.
Now, see Theorem 3, $F_{i+1/2}(t) = F(U_{i+1}(t)$, and F is Lipschitz continuous. Therefore, adding and subtracting $F(U_i(t)$, we obtain : $|E_h - G_h| \leq C'\ \Delta X$, where

$$G_h := \int_0^{+\infty} \sum_i \int_{I_i} F(U_i(t) \partial_X \phi(X,t) dX dt = \int_0^{+\infty} \int_{I\!R} \mathcal{U}_h(X,t) \partial_X \phi(X,t) dX dt$$

and $|C'| \leq T\ ||\partial_X \phi||_\infty .\ ||F'||_\infty .\ \sup_t \{\sum_i |U_{i+1}(t) - U_i(t)|\}$.
Finally, by compactness, G_h tends to B when $\Delta X \to 0$, which shows that U is a weak solution of (22). We would establish the entropy inequality in a similar way. First, when $\Delta t \to 0$ as in Theorem 3, the fully discrete entropy inequality (29) is preserved at the limit and provides the *semi-discrete* entropy inequality, i.e. a relation similar to (32), with U, $F(U)$ and the equality sign respectively replaced by $\eta(U)$, $q(U)$ and the same *inequality* sign as in (29), which implies the Lax entropy inequality by compactness as $\Delta X \to 0$.

□

Remark 5
In other words, at least in the homogeneous case $A = 0$, and away from vacuum, we have shown that the macroscopic system is the limit of a large number of vehicles on a long stretch of a highway and a large time scale of the same order. For a study of more general cases, we refer to reference [1]. We note by the way that in this limit situation the time-lag mentioned in the introduction vanishes.
In contrast, in the relaxed case $A > 0$, with a fixed constant A, we have to study the limit of (19) and (20) when the three parameters Δt, ΔX and ε tend to 0 together, with fixed ratios, and of course satisfy the CFL condition. So far, we have not studied this limit.

Remark 6
In terms of modeling, here we explicitly relate the semi-discretization of the macroscopic system to the microscopic system (1), *directly*, i.e without any intermediate kinetic description. Although we already mentioned the derivation of (5) from kinetic models, [11], our *direct* derivation is conceptually important: just imagine a similar result in gas dynamics ! For the relation between weak solutions in Eulerian and Lagrangian mass coordinates, we refer again to [20]. Finally, we have also learnt very recently of a preprint, [22], with exactly the same *formal* derivation of the same model.

5 Numerical methods and examples.

For numerical investigations we consider the equations in Eulerian and Lagrangian form. The time discretized microscopic equations (19, 20) or, equivalently, the Godunov method in Lagrangian coordinates (27), can be viewed as a particle method for the conservation law. Computing

$$\begin{aligned} \tau_i^{n+1} &= \tau_i^n + \lambda(v_{i+1}^n - v_i^n) \\ w_i^{n+1} &= w_i^n e^{\frac{-\Delta t}{T(\rho_i^{n+1})}} + (V(\rho_i^{n+1}) + P(\rho_i^{n+1}))(1 - e^{\frac{-\Delta t}{T(\rho_i^{n+1})}}) \end{aligned} \tag{33}$$

one obtains the location of the vehicles as follows:

$$x_i^{n+1} = x_i^n + \Delta t v_i^n. \tag{34}$$

The density in Eulerian coordinates at the point x_i is then given by the interpolation $\rho_i = \frac{\Delta x}{x_{i+1} - x_i}$. For discretization steps Δt and ΔX tending to 0 one obtains an approximation of the conservation law (5) in Eulerian coordinates. From the particle point of view this means that we have to increase the number of vehicles to obtain the desired approximation of the conservation law. However, one could as well use any other methods to resolve the limiting conservation law in Eulerian coordinates. For

example, any second order shock capturing scheme could be used for the macroscopic equations (5). Using such a scheme will lead to the same results as the solution of the above discrete equations with a large number of vehicles. We use a relaxation method as developed in [9]. The method is adapted to include the relaxation term on the right hand side of (5). This can be done in a straightforward way preserving the second order approximation.

In the following we will compare the microscopic particle approach and the above second order scheme using two test problems.
In all cases the equilibrium velocity $V = V(\rho)$ is chosen as a function fitting to experimental data:

$$V(\rho) = U(\frac{\rho}{\rho_m})$$

with

$$U(\rho) = v_m \frac{\pi/2 + arctan(11\frac{\rho - 0.22}{\rho - 1})}{\pi/2 + arctan(11 \cdot 0.22)},$$

where ρ_m is the maximal density and v_m the maximal velocity. The function $P(\rho)$ is chosen by setting $\gamma = 0$ and $\gamma = 1$, i.e. $m_2 = 1$ and $m_2 = 2$ respectively. In order to fulfill the subcharacteristic condition (9) we choose the function P as $P(\rho) = 2\ln(\rho/\rho_m)$ and $P(\rho) = 6\rho/\rho_m$. The first test problem is the following: We consider normalized quantities with maximal speed v_m equal to 1 and maximal density ρ_m equal to 1. From the macroscopic point of view we consider a Riemann problem with left and right states given by $\rho_L = 0.05, \rho_L v_L = 0.0025$, $v_L = 0.05$ and $\rho_R = 0.05, \rho_R v_R = 0.025$, $v_R = 0.5$. The discontinuity is located at $x = 0$. Note that $v_R > w_L = v_L + P(\rho_L)$. Thus, vacuum states appear during the evolution for the continuous conservation law for $\gamma = 1$, see [2].
The discretization size is chosen as $\Delta x = \Delta X = \frac{1}{40}$. This leads to an initial number of cars equal to 800. They are initial distributed equally spaced with the velocities 0.05 or 0.5 respectively. The time step is chosen according to the CFL condition.
Figure 4 shows density ρ and flux $q = \rho u$ at a fixed time for the particle and second order method for $\gamma = 1$ without relaxation term. Figure 5 shows the same for $\gamma = 0$. Figure 6 shows the evolution for $\gamma = 1$ with the relaxation term, where V and T are given by $V(\rho) = U(\rho)$ and $T(\rho) = \text{constant} = 20$. Figure 7 shows the same for $\gamma = 0$.

Finally, Figure 8 shows the results of our second test case, a more complicated situation: The evolution at a bottleneck at $x = 0$ is simulated. The number of lanes is reduced from three to two. This is achieved by setting the maximal density equal to the number of lanes. This means that the fundamental diagram is given by $V(\rho) = U(\frac{\rho}{\rho_m})$ where inside the bottleneck the maximal density ρ_m is reduced from 3 to 2. The boundary data on the left hand side are chosen such that the flux in the 3-lane region is slightly above the maximal possible flux in the two lane region which creates the traffic jam. ΔX and Δx are chosen as $\frac{1}{4}$ which yield a number of cars around 5000 during the evolution. Figure 8 shows the evolution for the microscopic

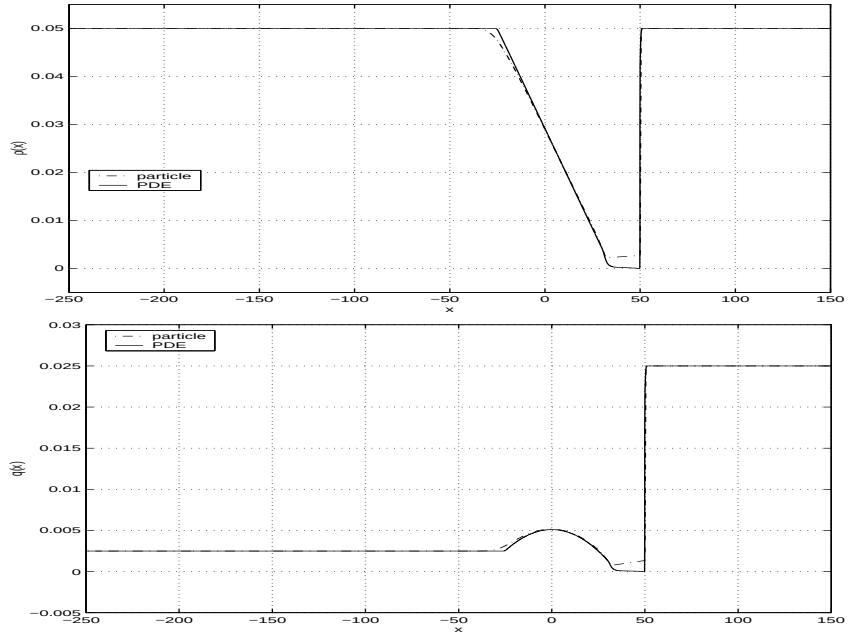

Figure 4: Time development of density and flux computed by particle method and second order method for $\gamma = 1$ without relaxation term.

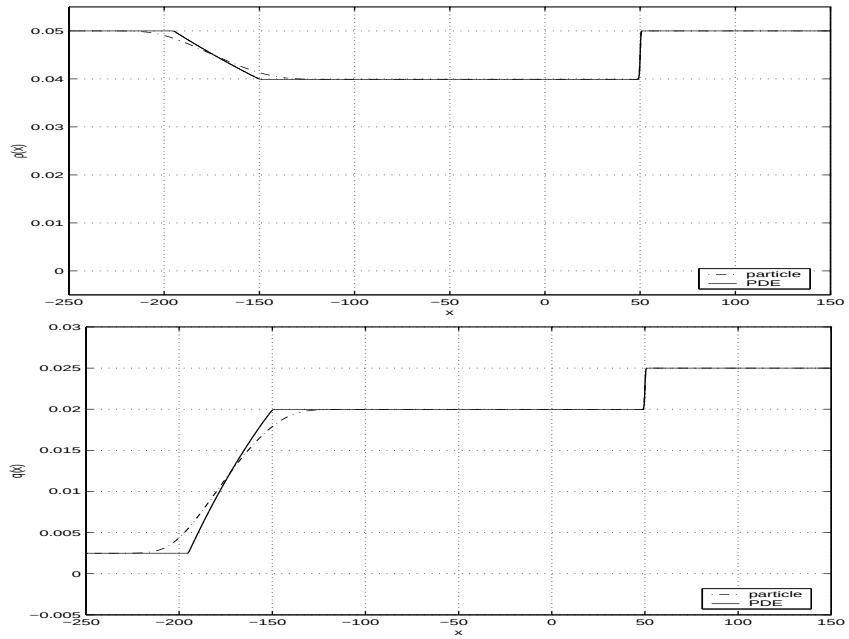

Figure 5: Time development of density and flux computed by particle method and second order method for $\gamma = 0$ without relaxation term.

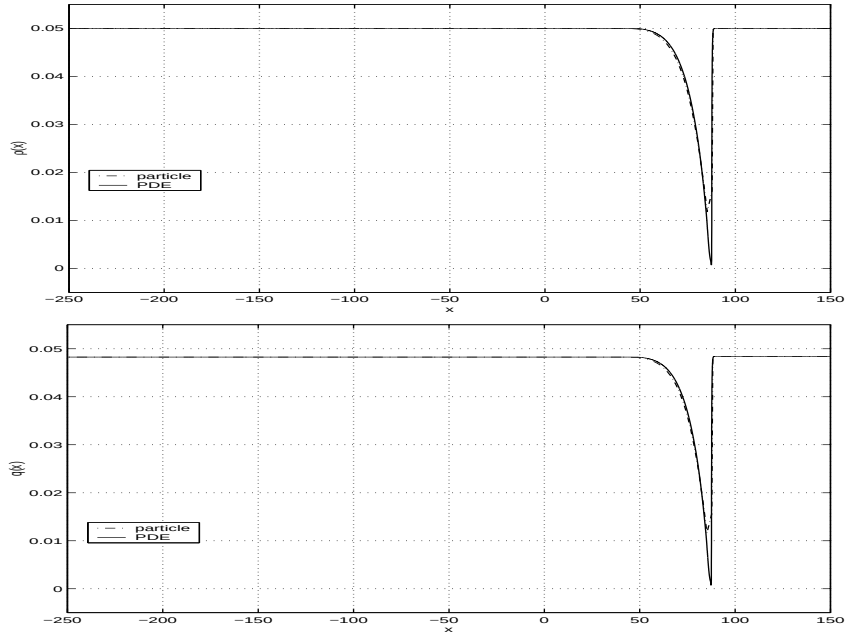

Figure 6: Time development of density and flux computed by particle method and second order method for $\gamma = 1$ with relaxation term.

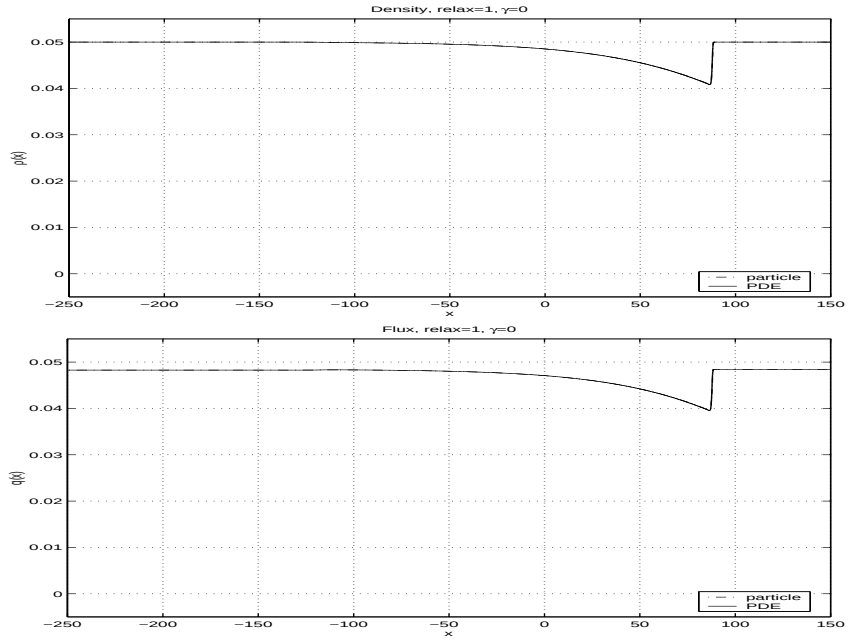

Figure 7: Time development of density and flux computed by particle method and second order method for $\gamma = 0$ with relaxation term.

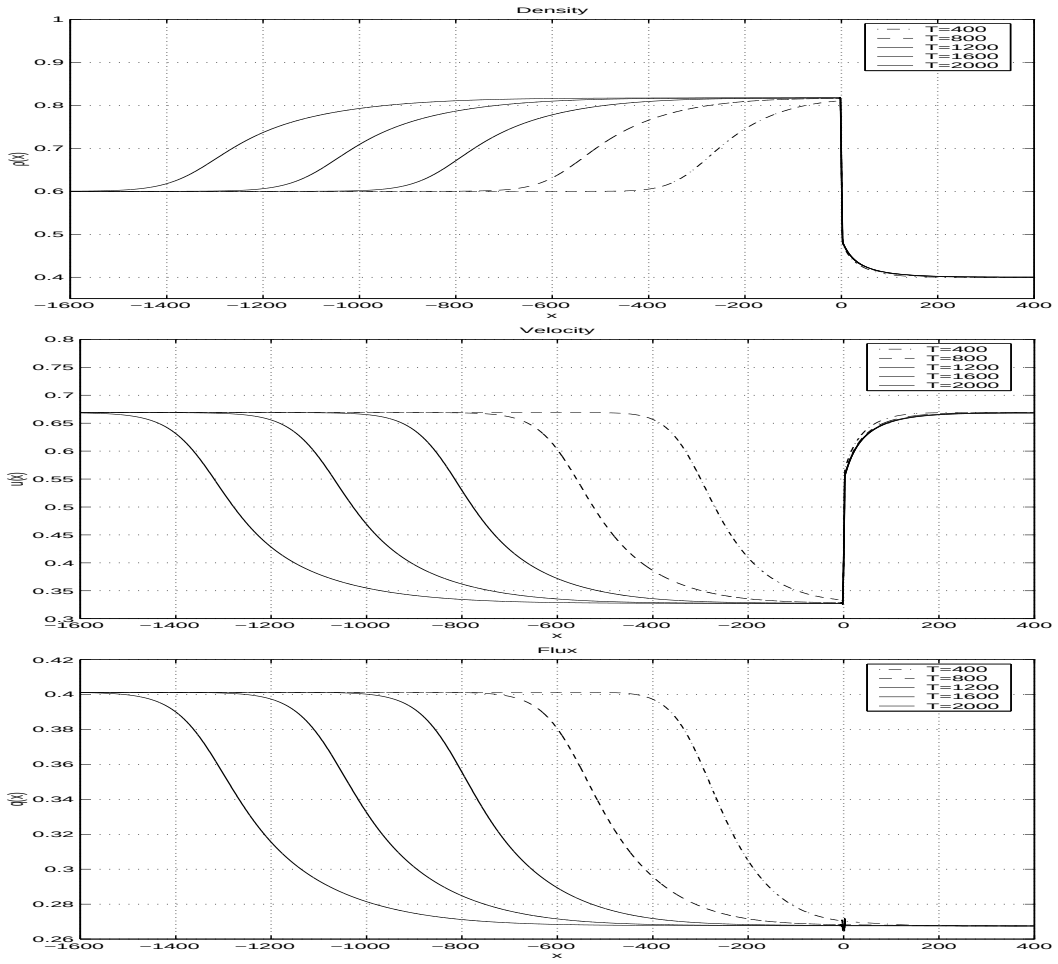

Figure 8: Time development of density, velocity and flux. Lane drop from 3 to 2 lanes at $x = 0$

particle method at different times. In particular, the development of a traffic jam is observed in the figure. Identical results are obtained if the second order method for the Eulerian equations is used.

Acknowledgments
The present work has been supported by the EC-TMR networks 'HCL' n° ERB FMRX CT 96 0033, and 'Asymptotic Methods in Kinetic Theory', n° ERB 4061 PL 97-0396, by Deutsche Forschungsgemeinschaft (DFG), KL 1105/5,and by the NSF-CNRS contract n° 5909.

References

[1] A. Aw. *Modèles hyperboliques de trafic automobile.* PhD thesis, Nice, 2001.

[2] A. Aw and M. Rascle. Resurrection of second order models of traffic flow? *SIAM J. Appl. Math.*, 60(3):916–938, 2000.

[3] G.Q. Chen and T.P. Liu. Zero relaxation and dissipation limits for hyperbolic conservation laws. *Comm. Pure Appl. Math.*, 46(5):755–781, 1993.

[4] R. Courant and K.O. Friedrichs. *Supersonic Flows and Shock Waves.* Springer, 1976.

[5] C.F. Daganzo. Requiem for second order fluid approximations of traffic flow. *Transportation Research B*, 29B:277–286, 1995.

[6] D.C. Gazis, R. Herman, and R. Rothery. Nonlinear follow-the-leader models of traffic flow. *Operations Res.*, 9:545, 1961.

[7] G.Q.Chen, C.D. Levermore, and T.P. Liu. Hyperbolic conservation laws with stiff relaxation terms and entropy. *Comm. Pure Appl. Maths*, 47(6):787–830, 1994.

[8] J. Greenberg. Extension and amplification of the aw- rascle model. *SIAM J. Appl. Math.*, 62(3):729–745, 2001.

[9] S. Jin and Z. Xin. The relaxation schemes for systems of conservation laws in arbitrary space dimensions. *Comm. Pure Appl. Math.*, 48:235–276, 1995.

[10] B. Keyfitz and H. Kranzer. A system of non-strictly hyperbolic conservation laws arising in elasticity theory. *Arch. Rat. Mech. Anal.*, pages 219–241, 1980.

[11] A. Klar and R. Wegener. Kinetic derivation of macroscopic anticipation models for vehicular traffic. *SIAM J. Appl. Math.*, 60:1749–1766, 2000.

[12] R.D. Kühne. Macroscopic freeway model for dense traffic. In N. Vollmuller, editor, *9th Int. Symp. on Transportation and Traffic Theory,VNU Science Press, Utrecht*, pages 21–42, 1984.

[13] P. D. Lax. Hyperbolic systems of conservation laws and the mathematical theory of shock waves. *Regional Series In Applied Mathematics.Philadelphia, Pa.: Soc. for Indus. and App. Math.*, V 11, of CBMS-NSF, SIAM 48p., 1973.

[14] R. Natalini. Convergence to equilibrium for the relaxation approximati ons of conservation laws. *Comm. Pure Appl. Math.*, 49:795–823, 1996.

[15] H.J. Payne. FREFLO: A macroscopic simulation model of freeway traffic. *Transportation Research Record*, 722:68–75, 1979.

[16] I. Prigogine and R. Herman. *Kinetic Theory of Vehicular Traffic.* American Elsevier Publishing Co., New York, 1971.

[17] M. Rascle. An improved macroscopic model of traffic flow: derivation and links with the lightill-whitham model. *Math. and Comp. Modelling*, 35(5-6), 2002.

[18] M. Schatzman. *Analyse numérique.* InterEditions, 1991.

[19] Blake Temple. Systems of conservation laws with coinciding shock and rarefaction curves. *Contemp. Math.*, 17 ,:pp 143–151, 1983.

[20] D. Wagner. Equivalence of the Euler and Lagrangian eqautions of gas dynamics for weak solutions. *J. Diff. Eq.*, 68:118–136, 1987.

[21] G.B. Whitham. *Linear and Nonlinear Waves.* Wiley, New York, 1974.

[22] M. Zhang. A non-equilibrium traffic model devoid of gas-like behavior. *Transp. Research Part B*, To appear.